International Conference on Smart Manufacturing Application
April. 9-11, 2008 in KINTEX, Gyeonggi-do, Korea

Cutting Force Simulation of Machining with Nose Radius Tools

B. Moetakef Imani[1] and N. Z.Yussefian[2]

[1] Department of Mechanical Engineering, Ferdowsi University, Mashhad, Iran
(Tel : +98-511-8615100; E-mail: imani@ferdowsi.um.ac.ir)
[2] Department of Mechanical Engineering, Ferdowsi University, Mashhad, Iran
(Tel : +98-511-6054664; E-mail: nima.zy@gmail.com)

Abstract: The mechanics of cutting with nose radius tools is discussed in the current paper. B-spline parametric curves are used to model the cutting edge and un-deformed chip area. The nose area is divided into elements which are normal to the elemental cutting edge. For the rest of the chip area the approach angle remains constant; thus, there is no need to subdivide this region and is considered as a single element. The elemental area and cutting edge contact length are found with an analytical algorithm for B-spline curves intersection. Cutting force is correlated to the chip area and cutting edge with cutting coefficients which are extracted from an orthogonal database. Accordingly, the elemental cutting force components can be computed. Summing up all the forces along the cutting edge provides the resultant cutting force. In addition, experimental cutting tests have been conducted to measure the cutting components along x-, y- and z-axis. The predicted results are in good agreement with experimental observations for a wide range of cutting conditions.

Keywords: Nose-Radius tool, Cutting-Force, B-spline representation of cutting edge

1. INTRODUCTION

Cutting force in machining process if not controlled may result in reduced tool life, poor surface finish and chatter vibrations. Hence, the prediction of cutting force for different cutting conditions has been always important to manufacturing engineers. In many machining operations cutting tools with nose radius are used. The tool nose radius and the variation of oblique angle along the cutting edge result in non-uniform distribution of the chip thickness. Therefore, the chip formation is a complicated 3D process. Numerous studies have been conducted on estimating the cutting force for nose radius tools [1-6]. In order to evaluate the cutting force, all the mentioned approaches were confined at least to one of the following limitations:

1- Empirical coefficients are obtained for a certain pair of tool and work piece and a limited range of cutting conditions.
2- True process geometry is not considered and it is replaced with equivalent cutting parameters and cutting edge representation.
3- The cutting edge geometry is limited to linear and circular segments, i.e. elliptic or Spline designs are not considered.

The main purpose of the current study is to develop a methodology for predicting the cutting force of nose radius oblique tools which is not confined to the above mentioned limitations.
Henceforth, the paper is organized as follows. In Section 2, the geometry of machining with a nose radius tool is discussed. The simulation methodology of machining with nose radius tools is then presented. The chip area is segmented into elements for which feed and approach angle can be considered constant. Section 3 describes the mechanics of cutting and proposes a method to compute the 3D cutting force components. The experimental setup is explained in Section 4 and in the following section, a comparison between predicted and measured cutting force components is made. Finally, Section 7 presents the conclusions of the paper.

2. GEOMETRIC MODELIG

2.1. Process Geometry

The geometry of machining by a tool with nose radius (r) is shown in Fig. 1. The straight side of the tool approaches the work piece with the side cutting edge angle (λ_L). The tool rake face is defined by two angles, namely side rake (α_s) and back rake (α_b) angles. The rake face may be flat or may have chip breakers. The cutting edge consists of side, end and nose segments. However, depending on cutting conditions, one or two of the above mentioned segments may not engage the cut. The un-deformed chip area depends on feed (c), radial depth of cut (DOC) and the tool geometry. It must be pointed out that the distribution of chip thickness is not uniform along the tool nose radius.

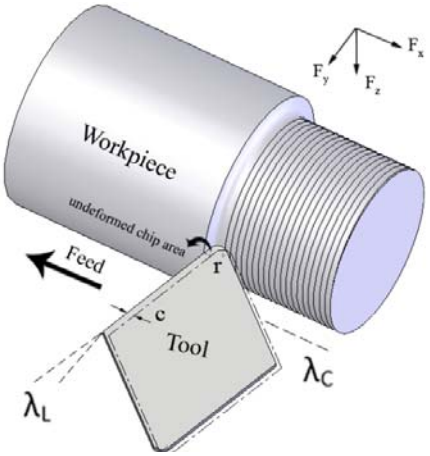

Fig.1. Geometry of metal cutting with nose radius tools.

It can be shown that at any desired point along the cutting edge, the local oblique angle i and the normal rake angle α_n can be evaluated by:

$$i = tan^{-1}[\tan(\alpha_s)\cos(\psi) - \tan(\alpha_b)\sin(\psi)] \quad (1)$$
$$\alpha_0 = tan^{-1}[\tan(\alpha_s)\sin(\psi) + \tan(\alpha_b)\cos(\psi)\ ] \quad (2)$$
$$\alpha_n = tan^{-1}[\tan(\alpha_0) * \cos(i)] \quad (3)$$

2.2. Geometric Simulation

For any cutting tool, regardless of edge geometric complexity, a series of points along the tool edge with certain increment are taken as input data points. A third degree clamped B-spline with uniform parameterization and knot span [7] is selected to interpolate input data points. The interpolated B-spline curve for the jth revolution is represented by:

$$C_x^j(u) = N(u).P_x \quad (4)$$
$$C_y^j(u) = N(u).P_y \quad (5)$$

where $[N]$ and $[P]$ are B-spline basis function and control point matrices, respectively. $C(u)$ represents the whole cutting edge where $u \in [0,1]$.

Two important parameters for nose radius tools defined as (see Fig.2 for details):

- u_{c1}: The corresponding parameter of the point at which the tool curvature begins (point B).
- u_{c2}: The corresponding parameter of the point at which the tool curvature ends (point D).

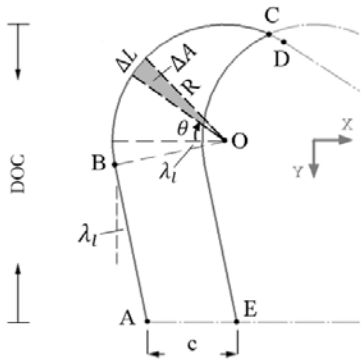

Fig.2. Simulation of cutting geometry (top view)

As the tool moves along the feed direction, the un-deformed chip area can be modeled considering two successive cutting edge locations, Fig. 2. If any geometric transformation is applied to a B-spline curve, the same result can be constructed by transforming its control points $[P]$. Therefore, the simulation of the tool movement along the feed direction as well as any other tool deflection can be obtained by an appropriate transformation applied to the B-spline control points [7]. Consequently the previous location of the cutting edge can be modeled by:

$$C_x^{j-1}(u) = N(u).[P_x + c] \quad (6)$$
$$C_y^{j-1}(u) = N(u).P_y \quad (7)$$

Considering the marginal line AE (Fig. 2) as a degree one B-spline, the required geometric parameters for the chip load calculations of these two successive locations can be classified as follows:

- u_{st}: The corresponding parameter of the point at which the edge engages the cut (point A).
- u_{int}: The corresponding parameter of the point at which the edge leaves the cut (point C).

$$A = \begin{bmatrix} C_x^j(u_{st}) \\ C_y^j(u_{st}) \end{bmatrix} \quad (8)$$
$$C = \begin{bmatrix} C_x^j(u_{int}^j) \\ C_y^j(u_{int}^j) \end{bmatrix} = \begin{bmatrix} C_x^{j-1}(u_{int}^{j-1}) \\ C_y^{j-1}(u_{int}^{j-1}) \end{bmatrix} \quad (9)$$

In order to find the u_{st} and u_{int} a special parametric curve intersection algorithm is developed. The main steps of the proposed algorithm are as follows. The B-spline curve which represents the tool edge is first subdivided into Bezier curves over its knot span. Then, the corresponding Bezier curves of two successive B-spline curves that might intersect are extracted using the strong convex hull property of B-splines. Lastly, the intersection point is found with an analytical method called algebraic pruning which is elaborated in [8].

Once the boundary of chip load is fully defined, the total chip area(A_t) and the total cutting edge contact length (L_t) can be evaluated by:

$$A_t = \int_{u_{st}}^{u_{int}^{j}} C_y^i(u)\frac{dC_x^j(u)}{du}du - \int_{u_{st}}^{u_{int}^{j-1}} C_y^{j-1}(u)\frac{dC_x^{j-1}(u)}{du}du \quad (10)$$

$$L_t = \int_{u_{st}}^{u_{int}^{j}} \sqrt{\left[\frac{dC_x^j(u)}{du}\right]^2 + \left[\frac{dC_y^j(u)}{du}\right]^2}\,du \quad (11)$$

The chip thickness and the approach angle change along the cutting edge, therefore the chip area should be segmented into elements of constant chip thickness and approach angle. The nose segment is subdivided into elements with respect to the local approach angle of the cutting edge ($\psi = \theta$), Fig.2. Using the proposed curve intersection algorithm, the elemental chip area (A_n) and elemental cutting edge contact length (L_n) for nose segment elements can be computed. For the rest of the chip area the approach angle and the chip thickness remain constant ($\psi = \lambda_l$), so this region is considered as a single element and the following equations hold:

$$\Delta A_l = A_t - \sum A_n \quad (12)$$

$$\Delta L_l = L_t - \sum L_n \quad (13)$$

where ΔA_l and ΔL_l are chip area and edge contact length for this element, respectively.

3. MECHANICS OF CUTTING WITH NOSE RADIUS TOOLS

In order to compute the cutting force, each element is considered as a single straight cutting edge. Cutting force is represented by tangential (F_t), feed (F_f) and radial (F_r) components, Fig.3. Experimental observations have shown that for a single straight oblique cutting edge, the cutting force components of F_t and F_r are independent of oblique angle [9] and the chip flow angle can be approximated by Stabler's chip flow rule [10].

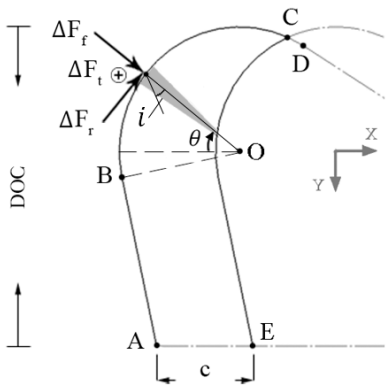

Fig.3. Cutting Force Computation

Since the chip thickness and approach angle change along the cutting edge, the magnitude and direction of elemental cutting forces vary. It is known that the resultant cutting force consists of two different constituents. The forces due to the chip removal process which are cutting forces and the forces due to the ploughing and rubbing of the cutting edge which are edge forces. Consequently each cutting force component has cutting and edge subcomponents. The cutting subcomponent is proportional to the chip area while edge subcomponent depends on cutting edge contact length. The cutting components can therefore be evaluated as follows [9, 11]:

$$\begin{aligned} \Delta F_t &= \Delta F_{tc} + \Delta F_{te} = K_{tc} * \Delta A + K_{te} * \Delta L, \\ \Delta F_f &= \Delta F_{fc} + \Delta F_{fe} = K_{fc} * \Delta A + K_{fe} * \Delta L, \\ \Delta F_r &= \frac{\Delta F_{tc}(\sin(i) - \cos(i)\sin(\alpha_n)\tan(\eta_c)) - \Delta F_{fc}\cos(\alpha_n)\tan(\eta_c)}{\sin(i)\sin(\alpha_n)\tan(\eta_c) + \cos(i)} \end{aligned} \quad (14)$$

where ΔA and ΔL are elemental chip area and cutting edge contact length, respectively. K_{tc} and K_{fc} are cutting coefficients and can be evaluated by:

$$K_{tc} = \tau_s \frac{cos(\beta_n - \alpha_n)}{sin(\phi_n)\,cos(\phi_n + \beta_n - \alpha_n)} \quad (15)$$

$$K_{fc} = \tau_s \frac{sin(\beta_n - \alpha_n)}{sin(\phi_n)\,cos(\phi_n + \beta_n - \alpha_n)} \quad (16)$$

Chip thickness ratio(r_t), shear angle(β), shear stress (τ_s) and edge coefficients (K_{te} and K_{fe}) are evaluated from orthogonal cutting database. ϕ_n is shear angle and can be evaluated by :

$$\phi_n = tan^{-1}\left(\frac{r_t\cos(\alpha_n)}{1 - r_t\sin(\alpha_n)}\right) \quad (17)$$

It is assumed that for each element, the Stabler's chip flow rule applies, that is the local oblique angle (i) equals the chip flow angle (η_c). Normal rake angle (α_n) and oblique angle i can be evaluated from Eqs.(1) ~ (3). Finally, the resultant forces for all elements can be computed by:

$$\begin{aligned} F_x &= \sum \Delta F_f cos(\psi) + \Delta F_r sin(\psi), \\ F_y &= \sum \Delta F_f sin(\psi) - \Delta F_r sin(\psi), \\ F_z &= \sum \Delta F_t, \end{aligned} \quad (18)$$

where ψ is the approach angle and equals to θ.

4. EXPERIMENTAL TESTS

Cutting tests have been conducted with carbide inserts on Al6061 T6 work piece material. Table 1 illustrates different cutting conditions of experimental tests. Cutting force components were measured with Kistler 9255b table dynamometer along with 5070 charge amplifier. A special tool holder had been designed and manufactured to mount the tool over the dynamometer, Fig. 4.

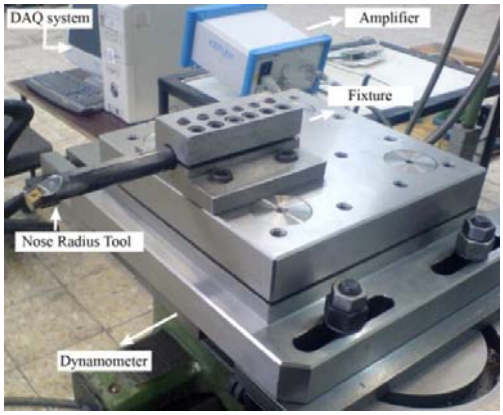

Fig.4. Experimental setup

Total of 192 cutting tests were conducted to obtain appropriate orthogonal database. More than 50 cutting tests were conducted to verify the proposed model.

Table 1.Cutting conditions of experimentations

Parameter	DOC (mm)	c (mm/rev)	V (m/min)	r (mm)	α_s (degree)	α_b (degree)	λ_l (degree)	λ_c (degree)
Range	0.1 - 4	0.02 - 0.14	70 - 100	0.4	-5	0	3	32

5. RESULTS AND DISCUSSION

Figures 5 to 7 compare predicted and measured cutting force components for c=0.14 mm/rev, V=100 m/min and DOC ranging from 0.1 to 4 mm.

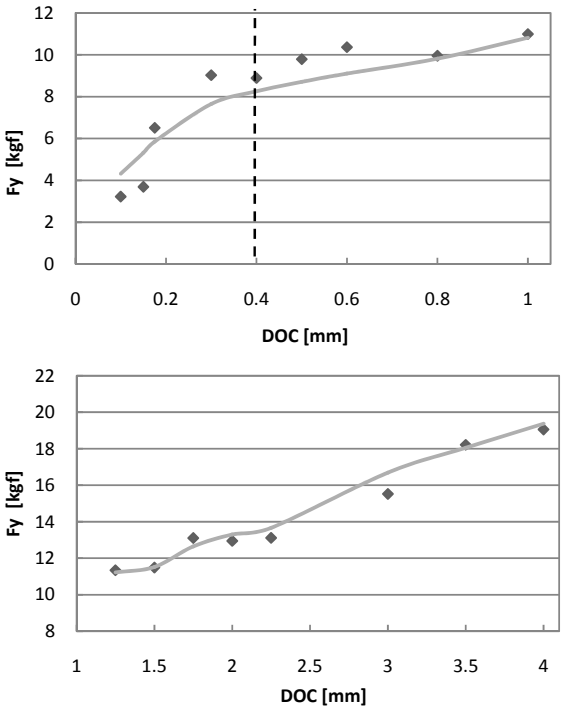

Fig.5.Predicted and measured F_y Component

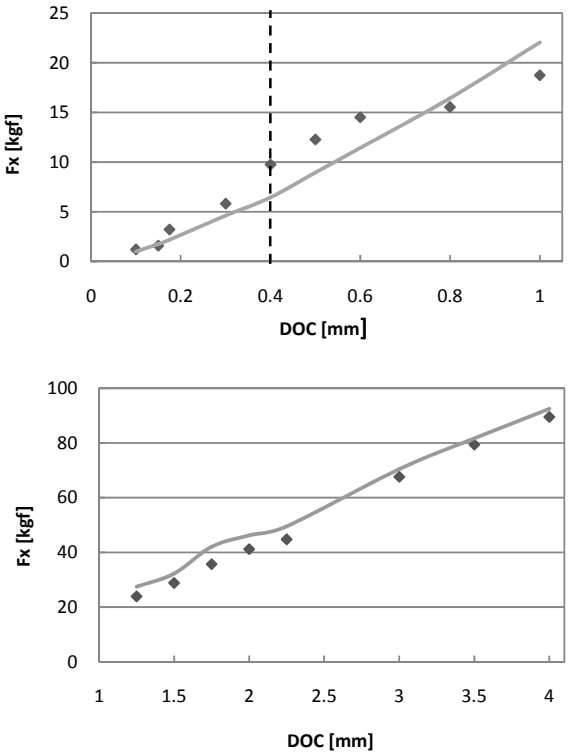

Fig.6.Predicted and measured F_x Component

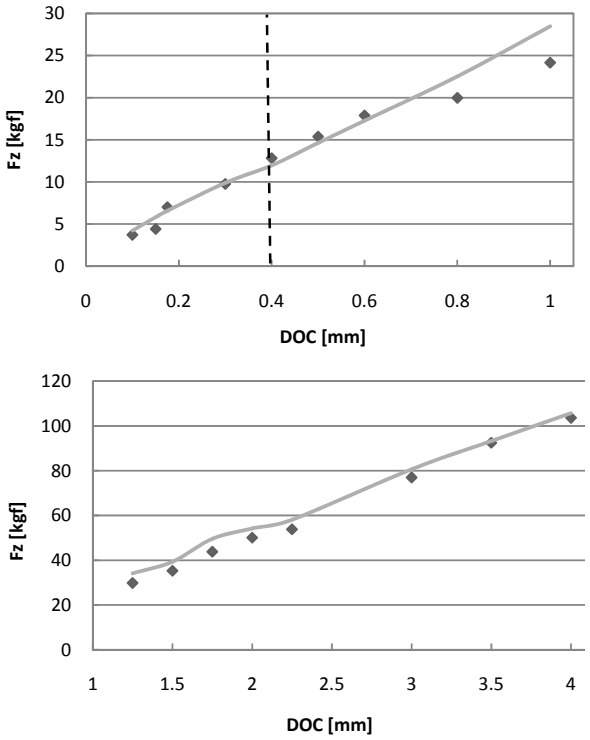

Fig.7.Predicted and measured F_z component

Measured forces are depicted by diamonds while solid lines represent predicted values. The dashed vertical line shows DOC value equal to r. As illustrated, the predicted and measured cutting forces are in good accordance for both roughing (DOC>R) and finishing (DOC<R) operations. F_x, F_y and F_z components are predicted with an average absolute error of -1.2, 4.81 and -5.21%, respectively.

5. CONCLUSION

The mechanics of cutting with a nose radius tool is discussed in the current article. By using B-spline parametric curves to simulate the cutting process, different cutting edge geometries can be modeled. A new method is proposed to evaluate the 3D cutting force components. Experimental cutting tests have been conducted. The comparison between the predicted and measured cutting force components, verify the validity of the proposed method.

REFERENCES

[1] L.V. Colwell, *Predicting the angle of chip flow for single point cutting tools,* Trans. ASME 76(1954)199-2028]

[2] H.T. Young, P. Mathew, P.L.B. Oxley, *Allowing for nose radius effects in predicting the chip flow direction, Cutting forces in bar turning*, Proc. Inst. Mech. Eng. 201 (C3) (1987) 213–226.

[3] J. Wang and P. Mathew, *Development of a General Tool Model for Turning Operations Based on a Variable Flow Stress Theory*, International Journal of Machine Tools Manufacture. Vol. 35. No. 1 pp. 71-90. 1995

[4] J.A. Arsecularatne, P. Mathew, P.L.B. Oxley, *Prediction of chip flow direction and cutting forces in oblique machining with nose radius tools*, J. Engng Manufact. (Proc. Inst. Mech. Engrs) 209 (1995) 305–315.

[5] J. A. ARSECULARATNE,t R. F. FOWLE and P. MATHEW. *NOSE RADIUS OBLIQUE TOOL: CUTTING FORCE AND BUILT-UP EDGE PREDICTION*. Int. J. Mach. Tools Manufact. Vol. 36, No. 5, pp. 585-595. 1996

[6] F. Atabey, I. Lazoglu, Y. Altintas. *Mechanics of boring processes—Part I*, Int. Journal of Machine Tools and Manufacture.

[7] Les Piegl, Wayne Tiller; *The NURBS Book*; New York: Springer-Verlag, 1997 ISBN: 3-540-61545-8.

[8] D. Manocha, Sh.Karishnan. *Algebric pruning: a fast technique for curve and surface intersection*, Comp. A. Geo. Design (1997) 823-845

[9] P.L.B. Oxley, The Mechanics of Machining: *An Analytical Approach to Assessing Machinability*, Ellis Horwood, England, 1989

[10] G.V. Stabler, *The fundamental geometry of cutting tools*, Proc. Inst. Mech. Engrs 165 (1951) 14–21.

[11] Y. Altintas, *Manufacturing Automation: Metal Cutting Mechanics,Machine Tool Vibrations and CNC, Design*, Cambridge University Press, 2000.